A New 3-D Open-Framework Zinc Phosphate $[C_6H_{16}N_2]\cdot[Zn_2(HPO_4)_3]$ Synthesized by a Solvothermal Combinatorial Approach

Yu Song,[a] Jihong Yu,*[a] Yi Li,[a] Min Zhang,[a] and Ruren Xu*[a]

Keywords: Solvothermal synthesis / Structure / Combinatorial approach / Host-guest systems / Zinc phosphate

By application of a combinatorial approach, a new open-framework zinc phosphate $[C_6H_{16}N_2]\cdot[Zn_2(HPO_4)_3]$ (denoted as phase **D**) has been obtained in the $Zn(OAc)_2\cdot2H_2O/H_3PO_4/N,N'$-dimethylpiperazine/ethylene glycol solvothermal reaction system at 180 °C. The factors influencing formation of the reaction products, such as crystallization temperature, solvent, as well as gel compositions, have been systematically studied. Phase **D** was characterized by X-ray powder diffraction, ICP, and TG analyses, and its structure was determined by single-crystal X-ray diffraction analysis. It crystallizes in the monoclinic space group $P2_1/n$ (no.14), with a = 8.6931(3) Å, b = 14.4394(5) Å, c = 12.6492(3) Å, β = 96.418(2)°, and Z = 4. It is composed of ZnO_4, $PO_3(OH)$ and $PO_2(OH)(=O)$ tetrahedral units linked by Zn–O–P bonds, forming an open-framework with intersecting eight-membered ring channels along the [100], [010], and [101] directions.

Introduction

Since pioneering work on the preparation of aluminophosphate molecular sieves by Wilson et al. in 1982,[1] open-framework metal phosphates have received much attention because of their great importance in many current fields of applied chemistry. This results from their catalytic and adsorptive properties, as well as optical, electronic and magnetic properties.[2–5] These materials are generally prepared under hydrothermal or solvothermal conditions in the presence of an organic amine as a structure-directing agent. A large number of metal phosphates (MePOs) with interesting open-framework structures have been obtained (Me = Al, Ga, In, Mn, Fe, Co, Ni, Zn, Sn, Ti, Zr, V, and Mo, etc.), amongst which open-framework zinc phosphates exhibit a vast structural diversity. To date, a large number of zinc phosphates have been prepared with 0-D cluster, 1-D chain, 2-D layer and 3-D open-framework structures.[6–16] Notable examples are the extra-large microporous compounds, such as ND-1 with 24-membered ring channels,[13] and $[H_3N(CH_2)_6NH_3][Zn_4(PO_4)_2(HPO_4)_2]\cdot3H_2O$ with 20-membered ring channels,[15] and the helical channel compounds, such as $[NH_3(CH_2)_2NH_2(CH_2)_2NH_3][Zn(PO_4)_3(HPO_4)]$[14a] which contains intersecting helical channels, and $[Zn_2(HPO_4)_4][Co(dien)_2]H_3O$ (dien = diethylenetriamine) with multidirectional helical channels.[16] The structures of these compounds are typically built up from tetrahedral ZnO_4 and PO_4 units, although in some cases ZnO_5 and ZnO_6 polyhedra exist. The structural variety is greatly enriched by the employment of various templating agents or structure-directing agents, such as organic amines, alkali metal cations and metal complexes.

Compared to the traditional synthesis methods for materials, the combinatorial approach has been proven as a high-throughput technique for the discovery of new materials. Following their application in the discovery of new drugs, combinatorial methods have been employed in many research areas, such as organic and inorganic chemistry, and biochemistry.[17–20] In recent years, a hydrothermal combinatorial method has been applied successfully in the syntheses of zeolites and related open-framework materials.[21–25] Akporiaye and co-workers first reported the application of a combinatorial strategy to the hydrothermal synthesis of zeolites using a multiple autoclave to perform at least 100 crystallizations under hydrothermal conditions.[21] Maier and co-workers modified the multi-autoclave so that the microgram-scale hydrothermal synthesis of TS-1 could be conducted in an array format on an Si wafer.[22] Bein and co-workers developed this methodology by introducing automatic identification of the products within the autoclave blocks.[23] By applying a hydrothermal combinatorial approach we have obtained three open-framework zinc phosphates including phases **A** $\{[C_6H_{16}N_2]_{0.5}\cdot[C_5H_{14}N_2]\cdot[Zn_6(PO_4)_5(H_2O)]\cdot3H_2O\}$ with sixteen-, ten- and eight-membered ring channels, phase **B** $[Zn_3(PO_4)_2(H_2O)]$ with eight-membered ring channels, and phase **C** $\{[C_4H_{14}N_2]\cdot[Zn_5(PO_4)_4(H_2O)]\}$.[24] Zhang et al. reported application of the combinatorial method to the synthesis of SAPO-34 by a vapor-phase transport technique.[25]

[a] State Key Laboratory of Inorganic Synthesis and Preparative Chemistry, College of Chemistry, Jilin University, Changchun 130012, P. R. China
Fax: (internat.) + 86-431-5168608
E-mail: jihong@mail.jlu.edu.cn
Supporting information for this article is available on the WWW under http://www.eurjic.org or from the author.

  DOI: 10.1002/ejic.200400216

Recently, we reported a new 2-D layered aluminophosphate $[C_2H_8N]_2{\cdot}[Al_2(HPO_4)(PO_4)_2]$ with a distinctive H-bonded helix formed by the organic amine templates and the inorganic network, prepared using a solvothermal combinatorial method.[26]

In this work, a new open-framework zinc phosphate $[C_6H_{16}N_2]{\cdot}[Zn_2(HPO_4)_3]$ from the $Zn(OAc)_2{\cdot}2H_2O/H_3PO_4$/*N*,*N*′-dimethylpiperazine/ethylene glycol reaction system has been obtained using the solvothermal combinatorial approach at 180 °C. The influence of various synthetic factors on the nature of the crystalline products, such as crystallization temperature, solvent type, as well as the gel compositions, has been systematically examined.

Results and Discussion

Using *N*,*N*′-dimethylpiperazine as the template and ethylene glycol as the solvent, a new phase **D** $\{[C_6H_{16}N_2]{\cdot}[Zn_2(HPO_4)_3]\}$ was crystallized from the $Zn(OAc)_2{\cdot}2H_2O/H_3PO_4$/*N*,*N*′-dimethylpiperazine/ethylene glycol system at 180 °C. Figure 1 shows its crystallization field. Pure phase **D** can be formed over a wide range at this temperature. Interestingly, if a certain amount of H_2O is added to the ethylene glycol, i.e., H_2O/ethylene glycol (1:4), phase **A** $\{[C_6H_{16}N_2]_{0.5}{\cdot}[C_5H_{14}N_2]{\cdot}[Zn_6(PO_4)_5(H_2O)]{\cdot}3H_2O\}$, with 16-membered ring main channels,[24] and phase **B** $[Zn_3(PO_4)_2(H_2O)]$, with eight-membered ring channels,[24] are formed. In addition, the range of formation for phase **D** becomes narrow. Furthermore, if 80% H_2O is added to the solvent mixture then no phase **D** is formed. Under this condition, the crystallization diagram is similar to that of the H_2O system at 180 °C, as reported previously.[24]

The powder X-ray diffraction pattern for phase **D** $\{[C_6H_{16}N_2]{\cdot}[Zn_2(HPO_4)_3]\}$ is shown in Figure 2, and is in agreement with the simulated XRD pattern generated from the single-crystal structural data of **D**, proving the phase purity.

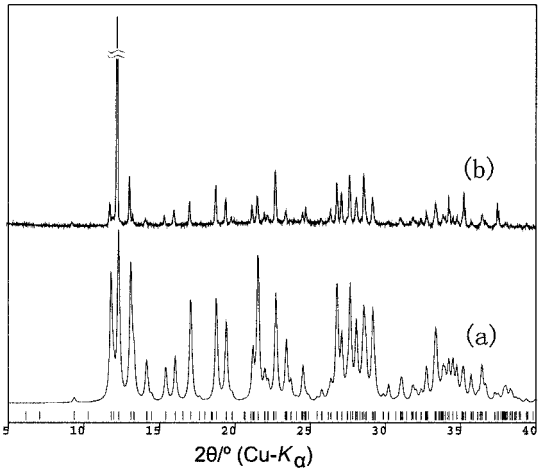

Figure 2. (a) Simulated and (b) experimental X-ray powder diffraction patterns of phase **D**

The influence of crystallization temperature was studied further. Upon reduction of the crystallization temperature to 140°C, phase **B** and an amine−phosphate cluster $([C_6H_{16}N_2]{\cdot}[H_2PO_4]_{0.5})$[28] (denoted as phase **E**), crystallize from the above system, and no phase **D** was obtained. As shown in Figure 3, phase **B** forms in the areas where $3 \leq P/Zn \leq 5$ and $3 \leq R/Zn \leq 7$ (R = *N*,*N*′-dimethylpiperazine), $4 \leq P/Zn \leq 5$ and $2 \leq R/Zn < 3$, with pH values of 7−9, while upon increase or decrease of the H_3PO_4 content, phase **E** begins to appear. Phases **B** and **E** coexist in the areas where $1 \leq P/Zn \leq 2$ and $1 \leq R/Zn \leq 7$, $6 \leq P/Zn \leq 7$ and $3 \leq R/Zn \leq 7$, and P/Zn = 3 and R/Zn = 3. Phase **E** forms in the areas where $3 \leq P/Zn \leq 5$ and $1 \leq R/Zn \leq 1.5$, and $6 \leq P/Zn \leq 7$ and $1 \leq R/Zn \leq 2$. On the other

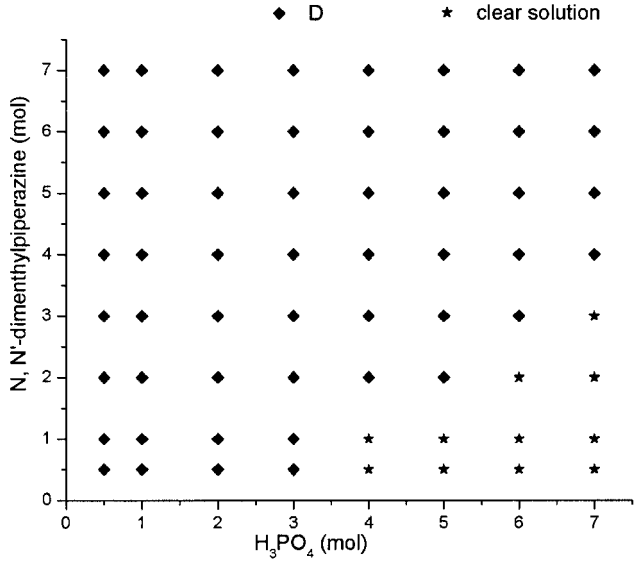

Figure 1. Crystallization field of phase **D** in the ethylene glycol system at 180 °C

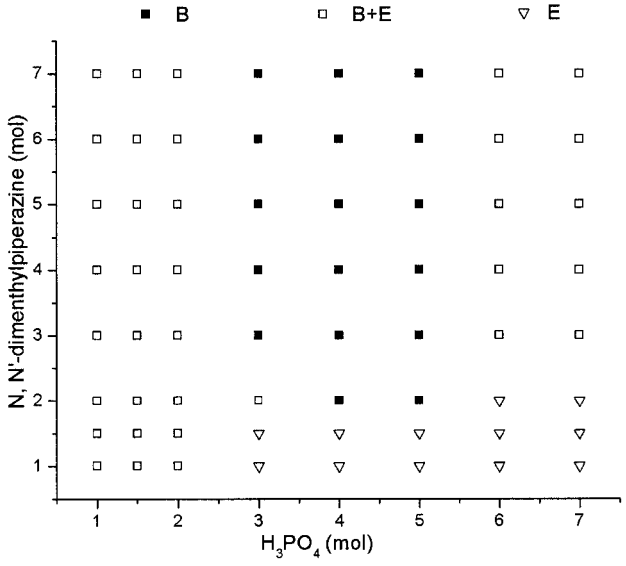

Figure 3. Crystallization field of phases **B** and **E** in the ethylene glycol system at 140°C

hand, when the the temperature was increased to 200°C, no crystalline product was obtained in the ethylene glycol system. However, phases **B** and **C** $\{[C_4H_{14}N_2]\cdot[Zn_5(PO_4)_4(H_2O)]\}$[26] are formed in the H_2O system at this temperature. Figure 4 shows its formation diagram. Phase **C** was obtained previously at 180 °C in the presence of trace amounts of transition metal cations, in the H_2O system.[24]

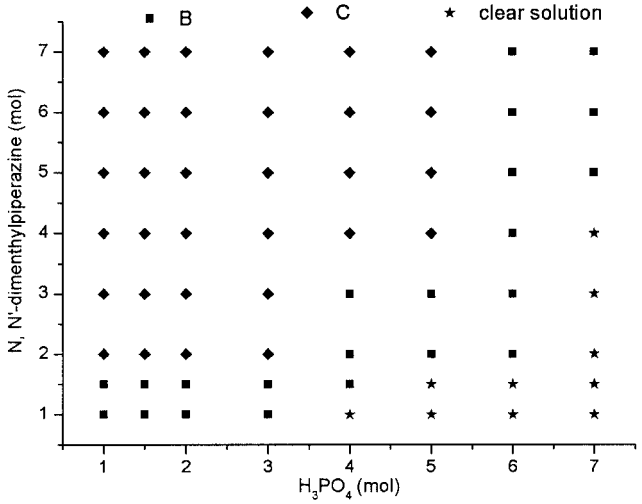

Figure 4. Crystallization field of phases **B** and **C** in the H_2O system at 200°C

Phase **D** $\{[C_6H_{16}N_2]\cdot[Zn_2(HPO_4)_3]\}$ crystallizes in the monoclinic space group $P2_1/n$ (no.14) with a = 8.6931(3) Å, b = 14.4394(5) Å, c = 12.6492(3) Å, β = 96.418(2)°, and Z = 4. As shown in Figure 5, each asymmetric unit contains 25 non-hydrogen atoms, of which 17 belong to the framework and eight to the guest molecules. There are two crystallographically independent zinc and three crystallographically independent phosphorus atoms. The Zn atoms are all tetrahedrally coordinated to oxygen atoms, and each makes four Zn−O−P bonds. The Zn−O bond lengths are in the range 1.922(2)−1.979(2) Å and the O−Zn−O bond angles are in the range 102.02(11)−114.99(11)°, which are typical for zinc phosphates.[6−16] The P atoms are tetrahedrally coordinated. P(1) and P(2) each share three oxygen atoms with adjacent Zn atoms. The $P-O_{bridging}$ bond lengths are in the range 1.509(3)−1.538(2) Å. The fourth P−O bond belongs to a P−OH group, with bond lengths of 1.574 (3) Å for P(1)−O(9)H and 1.572(3) Å for P(2)−O(10)H Å. The P(3) atom shares two oxygen atoms with adjacent Zn atoms. The P−O bond lengths are 1.504(3) Å for P(3)−O(3) and 1.499(3) Å for P(3)−O(8). The terminal O(11) and O(12) atoms are both disordered over two sites. P(3)−O(11) is a terminal P=O bond, while P(3)−O(12) is a terminal P−OH bond.

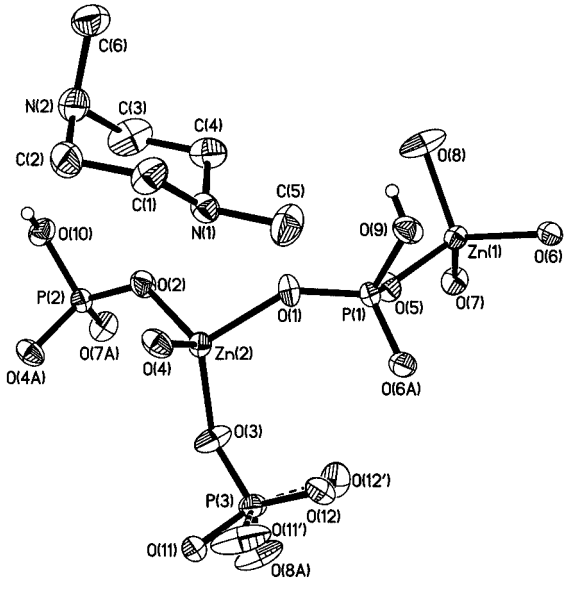

Figure 5. Thermal ellipsoid plot (50%) for **D** showing the atom labeling scheme

The alternation of ZnO_4, $PO_3(OH)$ and $PO_2(OH)(=O)$ tetrahedral units through Zn−O−P linkages forms an open-framework with eight-membered ring channels along the [100] direction (Figure 6), which are intersected with eight-membered ring channels along both the [010] and [101] directions. The 3-D open-framework can be viewed as a network of 4.8.12-net sheets parallel to the *ac* plane through O(7) atoms. This 4.8.12-net sheet is illustrated in Figure 7.

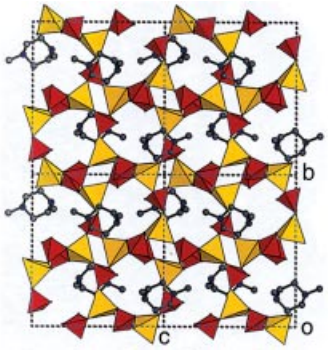

Figure 6. Polyhedral view of the framework structure of **D** viewed along the [100] direction showing the eight-membered ring channels (color code: Zn: yellow; P: red; C: grey; N: blue)

The balance of charge in the complex is achieved by diprotonation of *N*,*N*′-dimethylpiperazine. Each N atom of *N*,*N*′-dimethylpiperazine forms one H-bond to a framework oxygen atom. The N···O distances are in the range of 2.715(4)−3.015(5) Å.

Analysis of the structures of these phases gives some insight into the relative influence of various synthetic factors on the nature of the resulting crystalline products. In this work, the organic templating agent added to the initial reaction system for all the above compounds is *N*,*N*′-dimethylpiperazine. However, it was partially decomposed to *N*-methylpiperazine in phase **A**, which crystallized at 180°C in the H_2O system, and to *N*,*N*′-dimethylethylenediamine in phase **C**, which crystallized at 200°C in the H_2O system. It remained intact in phase **D** crystallized at 180°C in the ethylene glycol system and in phase **E** crystallized at 140

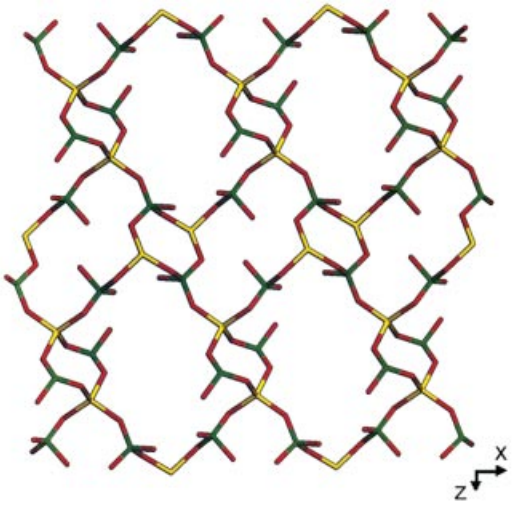

Figure 7. 4.8.12-net sheet parallel to the *ac* plane of **D** (color code: Zn: yellow; P: green; O: red)

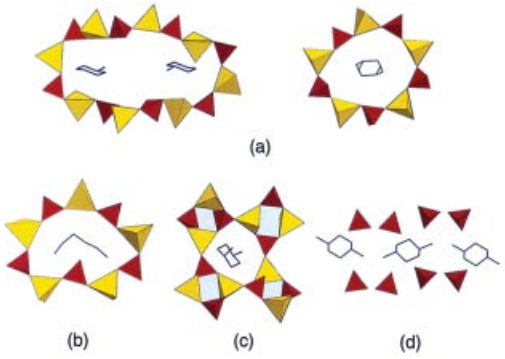

Figure 8. (a) The two diprotonated *N*-methylpiperazine molecules residing in the 16-membered ring channel viewed along the [100] direction and one diprotonated *N*,*N*′-dimethylpiperazine molecule residing in the 10-membered ring channel along [010] direction of **A**; (b) one diprotonated *N*,*N*′-dimethylethylenediamine molecule in the 10-membered ring channel of **C**; (c) one diprotonated *N*,*N*′-dimethylpiperazine molecule in the eight-membered ring channel of **D**; (d) structure of **E** containing a discrete zinc phosphate cluster and *N*,*N*′-dimethylpiperazine molecules (color code: Zn: yellow; P: red; C: grey; N: blue)

°C in the ethylene glycol system. Figure 8 (a−d) shows the templating molecules in the structures of phases **A**, **C**, **D** and **E**. It appears that *N*,*N*′-dimethylpiperazine is easily decomposed in the H_2O system at 180−200°C, but remains intact in the ethylene glycol system at 140−180°C. The above results indicate that the identities of crystallization products are strongly dependent on the organic amine species that are in turn affected by the crystallization temperature, as well as the solvent under solvothermal conditions.

Conclusions

A new open-framework zinc phosphate $[C_6H_{16}N_2]\cdot[Zn_2(HPO_4)_3]$ (phase **D**) with intersecting eight-membered ring channels has been obtained by applying a solvothermal combinatorial approach to the $Zn(OAc)_2\cdot 2H_2O/H_3PO_4/N,N'$-dimethylpiperazine/ethylene glycol system at 180°C. Factors such as gel composition, crystallization temperature and solvent, have significant influence on the resulting crystalline products. Four open-framework zinc phosphate phases **A** $\{[C_6H_{16}N_2]_{0.5}\cdot[C_5H_{14}N_2]\cdot[Zn_6(PO_4)_5(H_2O)]\cdot 3H_2O\}$, **B** $[Zn_3(PO_4)_2(H_2O)]$, **C** $\{[C_4H_{14}N_2]\cdot[Zn_5(PO_4)_4(H_2O)]\}$, **D** $\{[C_6H_{16}N_2]\cdot[Zn_2(HPO_4)_3]\}$, and an amine−phosphate cluster **E** $\{[C_6H_{16}N_2]\cdot[H_2PO_4]_{0.5}\}$, were obtained in the presence of the structure-directing agent *N*,*N*′-dimethylpiperazine in the H_2O or ethylene glycol systems. Our studies show that the state of the organic species, which is affected by the crystallization temperature and the solvent used, play an important role in the formation of the final crystalline products. This work further demonstrates that the combinatorial approach will assist greatly in the discovery of new open-framework materials and can improve our understanding of the factors that influence the crystallization of such materials.

Experimental Section

Synthesis and Characterization: The reactions were performed on the $Zn(OAc)_2\cdot 2H_2O/H_3PO_4/N,N'$-dimethylpiperazine/ethylene glycol or H_2O system in a multiautoclave with dimensions of 14 cm × 14 cm × 5.5 cm. The multiautoclave consists of a stainless steel block (3 cm in height) with 64 individual Teflon chambers (0.7 cm in diameter, 3.0 cm in depth, 800 μL in volume per chamber). Firstly, an aqueous or glycol solution of $Zn(OAc)_2$ was added to each Teflon chamber while they were mounted in a frame, using a Tecan CH Miniprep 75 pipette robot, followed by addition of *N*,*N*′-dimethylpiperazine (98.5%, ACROS) and H_3PO_4 (85 wt%). The reaction mixtures were shaken for homogenization using a vibration apparatus for 1 h. The 64 Teflon chambers were placed in the stainless steel block, then sealed by two stainless steel covers on top and bottom. Sixty-four individual Teflon covers (0.5 cm in thickness) were mounted on the top cover. The multiautoclave was heated in an oven at 140−200 °C for 60 h. After cooling, the arrays of Teflon chambers were put into a Hermle 2300 centrifuge apparatus for sample separation. The products were washed with deionized water followed by centrifugation several times. The products were dried at room temperature. The dried samples were transferred to a sample holder with 64 holes for automated X-ray analysis. Automated X-ray diffraction analysis was carried out with a computer-controlled *xyz* stage with a Bruker D8 Discover microdiffractometer with GADDS equipped with a CCD detector and using Cu-K_α radiation. Traditional X-ray diffraction analyses were performed with the X-ray diffraction (XRD) patterns collected with a Siemens D5005 diffractometer with Cu-K_α radiation (λ = 1.541 Å). Inductively coupled plasma (ICP) analyses were performed with a Perkin-Elmer Optima 3300DV spectrometer. Elemental analyses were conducted using a Perkin-Elmer 2400 elemental analyzer. Inductively coupled plasma (ICP) analysis showed that phase **D** contains 23.2 and 16.8 wt% of Zn and P, respectively (calcd. 24.3 and 17.4 wt%, respectively). The elemental analysis gave C, H and N contents of 13.8, 3.9 and 5.6 wt%, respectively (calcd. 13.5, 3.6 and 5.2 wt%, respectively). A NETZSCH STA 449C unit was used to carry out the thermogravimetric analysis (TGA) in air with a heating rate of 20°C/min. The occluded *N*,*N*′-dimethylpiperazine molecules decomposed at 200−450°C with a weight loss of 22.0 wt% (calcd. 22.2%).

Structure Determination: A suitable single crystal of phase **D** with dimensions 0.15 × 0.10 × 0.10 mm, was carefully selected under a polarizing microscope and glued to a thin glass fiber with cyanoacrylate (superglue) adhesive. The intensity data were collected with a Siemens diffractometer fitted with a Bruker SMART CCD detector, using graphite-monochromated Mo-K_α radiation (λ = 0.71073 Å). Data processing was done using the SAINT processing program. The structure was solved by direct methods and refined on F^2 by full-matrix least squares using SHELXTL97.[27] The Zn and P atoms were located first, and then the oxygen, carbon, and nitrogen atoms were located in the Fourier difference maps. O(11) and O(12) are disordered over two sites. The diprotonation of *N*,*N*′-dimethylpiperazine is suggested for the balance of charge. The hydrogen atoms on the amine molecules and in the P−OH bond were located geometrically. All non-hydrogen atoms were refined with anisotropic thermal parameters. The details of data collection and refinement are given in Table 1. Selected bond lengths and bond angles are listed in Table 2. CCDC-228303 contains the supplementary crystallographic data for this paper. These data can be obtained free of charge at www.ccdc.cam.ac.uk/conts/retrieving.html [or from the Cambridge Crystallographic Data Centre, 12 Union Road, Cambridge CB2 1EZ, UK; Fax: (internat.) + 44-1223/336-033; E-mail: deposit@ccdc.cam.ac.uk].

Table 1. Crystal data and structure refinement for phase **D**

Empirical formula	$C_6H_{19}N_2O_{12}P_3Zn_2$
Formula mass	534.88
Temperature	293(2) K
Wavelength	0.71073 Å
Crystal system, space group	monoclinic, $P2_1/n$
Unit cell dimensions	a = 8.6931(3) Å, α = 90° b = 14.4394(5) Å, β = 96.418(2)° c = 12.6492(3) Å, γ = 90°
Volume	1577.82(9) Å^{-3}
Z, calculated density	4, 2.252 Mg/m^3
Absorption coefficient	3.412 mm^{-1}
F(000)	1080
Crystal size	0.15 × 0.10 × 0.10 mm
θ range for data collection	2.15−23.26°
Limiting indices	$-9 \le h \le 9$, $-9 \le k \le 16$, $-14 \le l \le 13$
Reflections collected/unique	7342/2255 (R_{int} = 0.0388)
Completeness to θ = 23.36°	99.9%
Refinement method	full-matrix least squares on F^2
Data/restraints/parameters	2255/0/244
Goodness-of-fit on F^2	1.058
Final R indices [$I > 2\sigma(I)$][a]	R_1 = 0.0240, wR_2 = 0.0633
R indices (all data)	R_1 = 0.0292, wR_2 = 0.0652
Largest diff. peak/hole	0.435/−0.297e·Å^{-3}

[a] $R_1 = [\Delta F/(F_o)]$; $wR_2 = ([w(F_o^2 - F_c^2)])/[w(F_o^2)^2]^{1/2}$, $w = 1/\sigma^2(F_o^2)$.

Table 2. Selected bond lengths and angles for phase **D**

Bond lengths [Å]			
Zn(1)−O(7)	1.945(2)	Zn(1)−O(5)	1.948(2)
Zn(1)−O(6)	1.965(2)	Zn(1)−O(8)	1.972(3)
Zn(2)−O(1)	1.922(2)	Zn(2)−O(3)	1.925(3)
Zn(2)−O(2)	1.929(2)	Zn(2)−O(4)	1.979(2)
P(1)−O(5)	1.510(3)	P(1)−O(1)	1.511(3)
P(1)−O(6)[a]	1.531(3)	P(1)−O(9)	1.574(3)
P(2)−O(7)[b]	1.509(3)	P(2)−O(2)	1.513(2)
P(2)−O(4)[c]	1.538(2)	P(2)−O(10)	1.572(3)
P(3)−O(11′)	1.417(7)	P(3)−O(8)[d]	1.499(3)
P(3)−O(3)	1.504(3)	P(3)−O(12)	1.567(5)
P(3)−O(11)	1.607(6)	P(3)−O(12′)	1.629(6)
O(4)−P(2)[c]	1.538(2)	O(6)−P(1)[a]	1.531(3)
O(7)−P(2)[e]	1.509(3)	O(8)−P(3)[f]	1.499(3)

Bond angles [°]			
O(7)−Zn(1)−O(5)	104.94(11)	O(7)−Zn(1)−O(6)	112.24(11)
O(5)−Zn(1)−O(6)	114.99(11)	O(7)−Zn(1)−O(8)	114.33(11)
O(5)−Zn(1)−O(8)	104.24(12)	O(6)−Zn(1)−O(8)	106.06(12)
O(1)−Zn(2)−O(3)	113.39(12)	O(1)−Zn(2)−O(2)	102.02(11)
O(3)−Zn(2)−O(2)	114.34(11)	O(1)−Zn(2)−O(4)	104.27(11)
O(3)−Zn(2)−O(4)	112.94(11)	O(2)−Zn(2)−O(4)	108.89(11)
O(5)−P(1)−O(1)	110.76(15)	O(5)−P(1)−O(6)[a]	112.78(15)
O(1)−P(1)−O(6)[a]	111.49(15)	O(5)−P(1)−O(9)	108.97(14)
O(1)−P(1)−O(9)	108.26(15)	O(6)[a]−P(1)−O(9)	104.26(14)
O(7)[b]−P(2)−O(2)	113.17(15)	O(7)[b]−P(2)−O(4)[c]	110.54(15)
O(2)−P(2)−O(4)[c]	110.08(14)	O(7)[b]−P(2)−O(10)	105.50(15)
O(2)−P(2)−O(10)	108.33(14)	O(4)[c]−P(2)−O(10	109.02(14)
O(11′)−P(3)−O(8)[d]	116.2(3)	O(11′)−P(3)−O(3)	120.0(3)
O(8)[d]−P(3)−O(3)	111.19(16)	O(11′)−P(3)−O(12)	69.5(5)
O(8)[d]−P(3)−O(12)	121.1(3)	O(3)−P(3)−O(12)	113.4(2)
O(8)[d]−P(3)−O(11)	102.0(3)	O(3)−P(3)−O(11)	102.6(2)
O(12)−P(3)−O(11)	103.7(3)	O(11′)−P(3)−O(12′)	111.9(5)
O(8)[d]−P(3)−O(12′)	91.2(3)	O(3)−P(3)−O(12′)	101.4(3)
O(11)−P(3)−O(12′)	146.1(4)	P(1)−O(1)−Zn(2)	145.01(18)
P(2)−O(2)−Zn(2)	131.32(15)	P(3)−O(3)−Zn(2)	133.56(17)
P(2)[c]−O(4)−Zn(2)	130.08(15)	P(1)−O(5)−Zn(1)	133.83(16)
P(1)[a]−O(6)−Zn(1)	120.26(14)	P(2)[e]−O(7)−Zn(1)	137.35(17)
P(3)[f]−O(8)−Zn(1)	132.09(18)		

Hydrogen bonds	[Å]	[°]
O(9)−H(9)···O(11)[f]	2.574(7)	169.0
O(9)−H(9)···O(11′)[f]	2.573(7)	145.6
O(10)−H(10)···O(11)[c]	2.520(7)	164.2
O(10)−H(10)···O(11′)[c]	2.577(7)	143.7
N(1)−H(1)···O(4)	2.715(4)	171.9
N(2)−H(2)···O(8)[g]	3.015(5)	162.9

[a] Symmetry transformations used to generate equivalent atoms: $-x + 2, -y - 1, -z$. [b] $x - 1/2, -y - 3/2, z - 1/2$. [c] $-x + 1, -y - 1, -z - 1$. [d] $x - 1, y,$. [e] $x + 1/2, -y - 3/2, z + 1/2$. [f] $x + 1, y, z$. [g] $-x + 2, -y - 1, -z - 1$.

Acknowledgments

We are grateful to the National Natural Science Foundation of China and the State Basic Research Project (G2000077507) for financial support.

[1] S. T. Wilson, B. M. Lok, C. A. Messina, T. R. Cannan, E. M. Flanigen, *J. Am. Chem. Soc.* **1982**, *104*, 1146.
[2] A. K. Cheetham, G. Férey, T. Loiseau, *Angew. Chem. Int. Ed.* **1999**, *38*, 3268, and references therein.
[3] [3a] J. M. Bennet, W. J. Dytrych, J. J. Pluth, J. W. Richardson, J. V. Smith, *Zeolites* **1986**, *6*, 349. [3b] M. E. Davis, C. Saldarriaga, C. Montes, J. Garces, C. Crowder, *Nature* **1988**, *331*, 698. [3c] J. Yu, R. Xu, *Acc. Chem. Res.* **2003**, *36*, 481, and references therein.
[4] [4a] G. Férey, *Chem. Mater.* **2001**, *13*, 3084, and references therein. [4b] J. Yu, R. Xu, J. Li, *Solid State Sci.* **2000**, *2*, 181, and references therein.
[5] [5a] C. N. R. Rao, S. Natarajan, S. Neeraj, *J. Am. Chem. Soc.* **2000**, *122*, 2810, and references therein. [5b] R. Raja, G. Sankar, J. M. Thomas, *J. Am. Chem. Soc.* **2001**, *123*, 8153. [5c] S. Natarajan, *Chem. Commun.* **2002**, 780.
[6] [6a] J. Yu, Y. Wang, Z. Shi, R. Xu, *Chem. Mater.* **2001**, *13*, 2972.

[6b] W. Liu, Y. Liu, Z. Shi, W. Pang, *J. Mater. Chem.* **2000**, *10*, 1451.
[7] A. Choudhruy, S. Natarajan, C. N. R. Rao, *Inorg. Chem.* **2000**, *39*, 4295.
[8] S. B. Harmon, S. C. Sevov, *Chem. Mater.* **1998**, *10*, 3020.
[9] T. E. Gier, X. Bu, P. Feng, G. D. Stucky, *Nature* **1998**, *395*, 154.
[10] [10a] W. T. A. Harrison, M. L. Phillips, *Chem. Commun.* **1996**, 2771. [10b] W. T. A. Harrison, T. E. Gier, G. D. Stucky, R. W. Broach, R. A. Bedard, *Chem. Mater.* **1996**, *8*, 145.
[11] G. Alberti, M. Bartocci, M. Santarelli, R. Vivani, *Chem. Commmun.* **1996**, 2771.
[12] W. T. A. Harrison, M. L. F. Phillips, *Angew. Chem. Int. Ed. Engl.* **1995**, *34*, 1745.
[13] G. Yang, S. C. Sevov, *J. Am. Chem. Soc.* **1999**, *121*, 8389.
[14] [14a] S. Neeraj, S. Natarajan, C. N. R. Rao, *Chem. Commun.* **1999**, 165; *Chem. Mater.* **1999**, *11*, 1390; *New J. Mater.* **1999**, 23, 303; *J. Solid State Chem.* **2000**, *150*, 417. [14b] S. Ayyappan, X. Bu, A. K. Cheetham, S. Natarajan, C. N. R. Rao, *Chem. Commun.* **1998**, 2181. [14c] S. Ayyappan, A. K. Cheetham, S. Natarajan, C. N. R. Rao, *Chem. Mater.* **1998**, *10*, 3764. [14d] S. Natarajan, R. Vaidhanathan, C. N. R. Rao, S. Ayyappan, A. K. Cheetham, *Chem. Mater.* **1999**, *11*, 1633.
[15] A. R. Jennifer, T. A. H. William, *J. Mater. Chem.* **2000**, *10*, 2853.
[16] Y. Wang, J. Yu, M. Guo, R. Xu, *Angew. Chem. Int. Ed.* **2003**, *42*, 4089.
[17] Special issue: *Acc. Chem. Res.* **1996**, *29*, 112.
[18] G. Lowe, *Chem. Soc. Rev.* **1995**, *24*, 309.
[19] X. -D. Xiang, X. Sun, G. Briceno, Y. Lou, K. A. Wang, H. Chang, H. Chang, W. G. Wallace-Freedman, S. -W. Chen, P. G. Schultz, *Science* **1995**, *268*, 1738.
[20] J. N. Cawse, *Acc. Chem. Res.* **2001**, *34*, 213.
[21] [21a] D. E. Akporiaye, I. M. Dahl, A. Karlsson, R. Wendelbo, *Angew. Chem. Int. Ed.* **1998**, *37*, 609. [21b] D. Akporiaye, I. Dahl, A. Karlsson, M. Plassen, R. Wendelbo, D. S. Bem, R. W. Broach, G. J. Lewis, M. Miller, J. Moscoso, *Miroporous Mesoporous Mater.* **2001**, *48*, 367.
[22] [22a] J. Klein, C. W. Lehmann, H.-W. Schmidt, W. F. Maier, *Angew. Chem. Int. Ed.* **1998**, *37*, 3369. [22b] J. M. Newsam, T. Bein, J. Klein, W. F. Maier, W. Stichert, *Miroporous Mesoporous Mater.* **2001**, *48*, 355.
[23] K. Choi, D. Gardner, N. Hilbrandt, T. Bein, *Angew. Chem. Int. Ed.* **1999**, *38*, 2891.
[24] Y. Song, J. Yu, G. Li, Y. Li, Y. Wang, R. Xu, *Chem. Commun.* **2002**, 1720.
[25] L. Zhang, J. Yao, C. Zeng, N. Xu, *Chem. Commun.* **2003**, 2232.
[26] Y. Song, J. Yu, Y. Li, R. Xu, *Angew. Chem. Int. Ed.* **2004**, *43*, 2399.
[27] G. M. Sheldrick, *SHELXL Program*, version 5.1; Siemens Industrial Automation, Inc., Madison, WI, **1997**.
[28] A. Choudhury, S. Natarajan, C. N. R. Rao, *J. Chem. Soc., Dalton Trans.* **2000**, 2595.

Received March 18, 2004
Early View Article
Published Online July 12, 2004

